

Suitability of magnetometry to detect clandestine buried firearms from a controlled field site and numerical modeling



Elijah Achuoth Deng^a, Kennedy O. Doro^{b,*}, Carl-Georg Bank^a

^a Department of Earth Sciences, University of Toronto, 22 Russell Street, Toronto, Ontario M5S3B1, Canada

^b Department of Environmental Sciences, University of Toledo, 2801 West Bancroft Street, Toledo, OH, 43606-3390, USA

ARTICLE INFO

Article history:

Received 26 January 2020

Received in revised form 15 June 2020

Accepted 30 June 2020

Available online 2 July 2020

Keywords:

Forensic science

Forensic geophysics

Magnetic

Gradiometry

Controlled geophysical research

Detecting buried weapons

ABSTRACT

The detection of buried firearms remains a critical issue in law enforcement. We assess the suitability of magnetic gradiometers to detect buried rifles and handguns at multiple depths using numerical modeling and field investigations. Our simulation is based on a simple approach to characterize handguns and rifles as long magnetic dipoles with the firearm characterized by its magnetization, length, centre, azimuth and plunge which allows us to calculate their total magnetic field and gradient anomalies. We compare these synthetic data to field gradiometer data collected with a Gem Systems GSM-19GW Overhauser magnetometer at a field site near Toronto, Canada, where six firearms are buried. Our field magnetometer consists of two sensors with a relative vertical separation of 0.55 m. We measure the largest anomaly (± 20 nT) for a rifle at 0.6 m depth, and the smallest anomaly (± 2 nT) for a handgun buried at 1.8 m depth. The measured anomalies spatially coincide with the locations of weapons while dipole anomalies align along the orientation of the firearms. Our modeling results show that vertically buried weapons produce significantly stronger anomalies than horizontal ones, and even slight tilts enhance the anomalies. We recommend a 0.25 m grid spacing to search for weapons using magnetometry. Our study shows that a range of firearms buried up to 1.8 m can be detected, suggesting that gradient magnetometers are useful tools in forensic weapon searches.

© 2020 Elsevier B.V. All rights reserved.

1. Introduction

Law enforcement agents are often faced with the daunting task of searching for clandestine burials of illegal weapons, including guns, explosives and other harmful objects as part of forensic investigations to unravel criminal acts or intentions and to ensure justice for victims [1–3]. While these forensic targets are shallow, typically within three meters below the subsurface [1], locating them by trial and error excavations without useful hints could be costly and labor intensive even for small search areas like back yards. Search teams have relied on personal experience [1], the use of specially trained sniffer dogs [4] and hints from other approaches, including geomorphological analysis [5], to obtain leads for further investigation. Shortages in manpower, varying chances of success using trained dogs, and increasing sophistication in planning and carrying out the associated crime, limit reliance on these approaches alone for investigative leads [6].

Geophysical methods, which image the shallow subsurface at a high resolution, provide non-destructive alternative approaches for forensic searches [7,8]. Geophysical measurements are relatively fast and allow for wide spatial coverage within a short period of time. Apart from qualitative information based on measured anomalies, quantitative analysis of measured signals also provides information on coordinates, magnitudes and other properties of the target that could provide a more specific guide to subsequent forensic intrusive investigation [9,10].

As in other shallow subsurface geophysical investigations, the use of geophysical techniques for forensic searches rely on measured property contrasts between the target object and the surrounding soils, including electrical conductivity (or its inverse - resistivity), dielectric permittivity, magnetic susceptibility and seismic velocities (see [8,11] for background). Forensic investigations have used ground penetrating radar [1,12,13], electrical resistivity tomography [14,15], electromagnetics [16], magnetometry [17,18] and seismic surveys [19]. Most of these have been on clandestine graves, with a few studies targeting buried weapons (e.g. [13,18]).

Weapons used for criminal activities which could be buried to conceal the criminal act or intentions include a variety of objects, for example: handguns, rifles, knives, axes, sharp edge metals or

* Corresponding author at: Department of Environmental Sciences, University of Toledo, 2801 West Bancroft Street, Mail Stop # 604, Toledo, OH, 43606-3390, USA.

E-mail address: kennedy.doro@utoledo.edu (K.O. Doro).

explosives [1,2]. Forensic searches for weapons with high metallic content have routinely involved the use of metal detectors which measure secondary electromagnetic fields created by the interaction of the transmitted primary electromagnetic fields with the metallic object being searched for [20,21]. Some research has attempted to determine the depth to targets, for example by taking measurements at different heights [22] or by robot-assisted scanning of an area [23]. While using metal detectors is quick and does not require a high level of training, false anomalies have limited their use and have prompted interest in testing other geophysical techniques [24,21]. A major recent research project involved a field assessment of multiple geophysical methods including ground penetrating radar, electromagnetics and magnetism for locating real firearms at a controlled test site in Orlando, Florida. This research detected steel rifles down to 0.75 m (deepest burial) and handguns to less than 0.50 m with a Schonstedt GA-72Cd magnetic locator [2]. At the same research site a Geonics EM-38 conductivity meter found similar detection limits [21], while surveys with a Fisher M-97 metal detector resulted in even shallower detection limits [25]. According to these studies, ground penetrating radar and electromagnetics-based metal detectors successfully detected buried weapons but at shallow depths. Magnetometry, in contrast, shows promise in detecting weapons at greater depths.

Metal detectors, conductivity meters, and ground-penetrating radar need to produce their own signal which limits their depth penetration; in contrast, magnetometry measures changes in Earth's natural magnetic field [8] and has thus the potential to detect buried weapons at greater depth, provided the property contrast between the target and the soil surrounding it is large enough. Its widely reported success in archeological studies (for a recent review see [9]), provides an additional impetus to explore this approach further for forensic investigation. Metal parts have the highest magnetic susceptibility of artefacts found in soils [26], and firearms also tend to maintain remanent magnetism [27]. However, some metals - like copper that may be used in alloys, and even high-grade stainless steel - are non-magnetic, rendering this method less useful [28]. As a consequence, the literature reports mixed results on applying magnetic based methods for detecting buried weapons. For example, a study by Hansen and Pringle [29] buried a replica handgun 0.15 m below a concrete patio and reports that a Geonics FM15 fluxgate gradiometer did not detect it, while a Gem Systems GSMP-40 potassium-vapour gradiometer did. Another study using a Geoscan FM256 fluxgate gradiometer was able to find buried replica handguns at shallow depths to 0.5 m [28]. These contrasting results show the knowledge gap including the optimum detection depths, effect of sensor configuration, geology and other environmental factors on measured magnetic signals in relation to detecting buried weapons; hence the need to test this method in different environments.

Information about coordinates and depth of a target cannot easily be extracted from magnetic data due to the inherent non-uniqueness of the method [8]. Several approaches seem promising, for example equivalent dipole [30], extended Euler deconvolution [31], analytical signal for single dipole or a line of dipoles [32], or tilt-depth method across a vertical boundary [33]. All of these have to make simplifying assumptions, for example that the object can be approximated by a point dipole or that the magnetization is purely induced and thus aligned with Earth's field at the survey location. This study proposes an easy forward modeling approach to match magnetic total field or vertical gradient data. Vertical magnetic gradiometers, which measure the difference between two magnetic sensors at fixed vertical separation, are able to highlight magnetic signatures from shallow targets [34].

The aim of our study is to employ investigations at a controlled field site and numerical modeling to assess the suitability of using

magnetic gradiometers to detect buried rifles and handguns. We first calculate synthetic magnetic total field and gradiometer data using formulas for a long dipole which we think adequately describes the field of a "long gun" in a shallow burial. We then compare model results to data collected in a field study which surveyed real buried firearms. Finally, we assess the detection limits, specifically the maximum burial depth at which firearms such as those used in our study may be detected by a magnetic gradiometer.

2. Method

Magnetometry measures small perturbations or "anomalies" in the local earth's total magnetic field which can be associated with the presence of a ferromagnetic objects (in this case either the rifle or handgun). Standard magnetic measurements using a single magnetometer require correcting for temporal and regional variation in the earth's magnetic field including effects of diurnal variations, micro-pulsation, magnetic storms and other transient magnetic effects originating outside the earth's field [8]. This correction can be done either by setting up a fixed base magnetometer where repeated measurements are taken to establish a background trend in comparison to the field data, or by the use of tie lines. As an alternative, the vertical gradient of the total magnetic field can be measured which uses two sensors at a fixed separation to determine the difference between them and the separation determines the depth of investigation [8,35–37]. Such gradient data automatically excludes both temporal and regional variations in the Earth's magnetic field during the duration of a survey, in contrast to total field data. Using a small separation between sensors also enhances near surface signals which are typically weak and could be masked by deeper sources while the spatial resolution is significantly improved compared to total field measurement alone.

2.1. Numerical modeling

Several approaches have been developed to forward model magnetic data. Profile data can be simulated for buried 2D objects with an arbitrary cross-section [38], while 3D data can be calculated assuming simple objects like spheres or prisms below ground [39] or by dividing the subsurface into regular prismatic cells [37,40] or arbitrary meshes [41]. Sometimes these methods will only allow induced magnetization. Given that firearms have a small cross-section and tend to be elongated we suggest a simple approach to model handguns and rifles as long magnetic dipoles.

Simple dipole models for interpreting measured magnetic anomalies [30,35,36] are inadequate to calculate the field of a rifle because if it is buried within a few meters of the subsurface then the distance between the measuring sensor and some part of the firearm may be similar to or even smaller than the length of the firearm. In our model, we simplify the firearm to be a long rod and although it may have both induced magnetization and remanent magnetization (resulting from mechanical stress during production or firing), we assume that both point along the axis of the barrel and are thus indistinguishable from one another. Parameters describing the weapon are thus its length and magnetization, as well as the location of its center in the subsurface and the azimuth (angle to North) and plunge (angle from the horizontal).

Our modeling of magnetic maps for buried weapons extends earlier work by Seleznyova et al. [42–44] who derive equations for the total magnetic field of a long dipole by superposition of the fields of two magnetic monopoles. They use cylindrical coordinates that take advantage of the radial symmetry of the dipole field. Our extension of this model is summarized in Fig. 1 and involves two steps. First, we apply vector algebra to convert the cylindrical

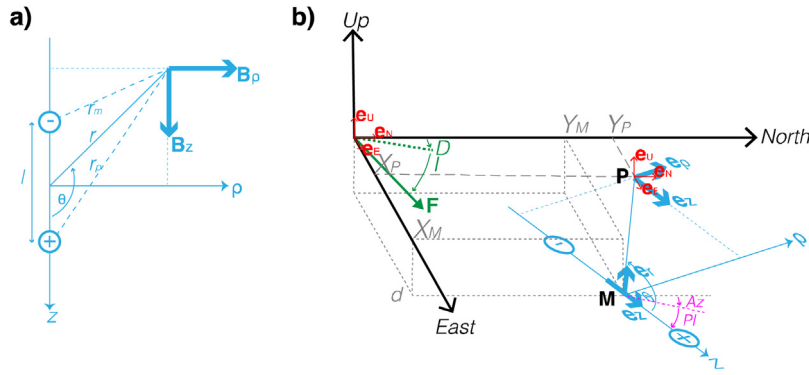


Fig. 1. Magnetic anomaly calculation. (a) Radial and vertical components B_ρ and B_z of magnetic field for a long-dipole, modified from Fig. 3 in [42]. (b) Placement of this cylindrical coordinate system into a more practical cartesian coordinate system and calculation of converted field components.

coordinates - which are based on the distance of the measurement point to the center of the dipole and the angle of the line connecting these two points to the dipole axis - into a cartesian coordinate system with its axes pointing North, East, and vertical up. This system better resembles the coordinates we use to collect data in a magnetic survey. Second, we use the principle of superposition and simple vector addition to add this converted magnetic field of the buried dipole to the Earth's background field that is reported in the same coordinate system. An added benefit of reporting a dipole field in cartesian coordinates is that it also allows us to calculate the combined field of several objects buried on the same site.

Seleznyova et al. [42, equation 26] define the radial component of the magnetic field of a long dipole as:

$$B_\rho = \frac{\mu_0}{4\pi} \cdot \frac{m}{l} r \sin\theta \left(\frac{1}{r_p^3} - \frac{1}{r_m^3} \right)$$

and its vertical component as:

$$B_z = \frac{\mu_0}{4\pi} \cdot \frac{m}{l} r \cos\theta \left(\frac{1 - \frac{1}{2}l}{r_p^3} - \frac{1 + \frac{1}{2}l}{r_m^3} \right)$$

where μ_0 is the permeability of a vacuum; m the strength of magnetic dipole [Am^2]; l the length of dipole [m]; θ the polar angle between the direction of the dipole and the line connecting the observation point P to the centre of the dipole; r the distance between this observation point and the centre of the dipole; and r_p and r_m are distances between this observation point and the ends of the dipole (Fig. 1a).

The converted coordinate system is described by the Cartesian coordinates $\mathbf{e}_E, \mathbf{e}_N, \mathbf{e}_U$ pointing East, North and Up (Fig. 1b), and we can express the unit coordinate vectors of the cylindrical system in this new coordinate system as follows:

Defining d as the depth to the dipole centre and \mathbf{M} as the location of the centre of the dipole at (X_M, Y_M, d) , and defining azimuth Az (clockwise from North) and plunge Pl (positive downward) of the dipole we convert the magnetization direction by

$$\mathbf{e}_z = \begin{pmatrix} \sin Az & \cos Pl \\ \cos Az & \cos Pl \\ -\sin Pl \end{pmatrix}$$

which allows us to obtain the endpoints of the dipole as $M_p = \mathbf{M} + \frac{1}{2} \mathbf{e}_z$ and $M_m = \mathbf{M} - \frac{1}{2} \mathbf{e}_z$.

To calculate the radial direction, we first obtain \mathbf{e}_r as the direction from \mathbf{M} to \mathbf{P} , the measurement point at $(X_P, Y_P, 0)$: $\mathbf{e}_r = \frac{1}{r} (\mathbf{P} - \mathbf{M})$ and the distance between those points as $r = \sqrt{(\mathbf{P} - \mathbf{M}) \cdot (\mathbf{P} - \mathbf{M})}$. The distances from the end points of the dipole to the measurement point are computed in an equivalent way. We

calculate the polar angle $\theta = \cos^{-1}(\mathbf{e}_z \cdot \mathbf{e}_r)$ via the dot product and the radial direction

$$\mathbf{e}_\rho = (\mathbf{e}_z \times \mathbf{e}_r) \times \mathbf{e}_z$$

This gives us all the information we require to compute the cylindrical field components of the magnetic field of the long dipole and convert those into cartesian coordinates:

$$\mathbf{B} = B_\rho \mathbf{e}_\rho + B_z \mathbf{e}_z$$

The local geomagnetic field, given its total field strength F, declination D, and inclination I, can be written in the cartesian coordinate system as

$$\mathbf{F} = F \begin{pmatrix} \sin D & \cos I \\ \cos D & \cos I \\ -\sin I \end{pmatrix}$$

The perturbation or total field anomaly \mathbf{A} is computed by subtracting the dipole field vector from the local geomagnetic field vector:

$$\mathbf{A} = \mathbf{F} - \mathbf{B}$$

To simulate gradiometer data, we subtract the values of the total field anomaly calculated at two elevations; an example of measurements at two elevations and their difference is shown in Fig. 2.

Representative examples of modeled data for different depths, different orientations, and different lengths of dipoles are shown in Fig. 3. In these calculations we approximate a rifle to be 1.0 m long with a magnetization of 0.5 Am^2 , while a handgun is 0.1 m and has a magnetization of 0.05 Am^2 . Our examples use approximate values of the background magnetic field for a location just to the Northwest of Toronto with a magnetic field strength of 54 mT, declination of 10 degrees West, and an inclination 70 degrees [45].

The modeling results (Fig. 3) allow us to make four statements: (i) Deeper dipoles will give rise to smaller but broader anomalies measured at the surface as expected. (ii) A long dipole will create spatially separate anomalies compared to a short dipole, especially noticeable at shallow burials. The separation between maximum and minimum value can provide an indication of dipole length while taking the depth of the object into account. (iii) Changing the plunge of the dipole increases either the positive or the negative anomaly, depending which of them rotates closer to the surface, and even at intermediate plunge (20 degrees) this anomaly becomes prominent. At shallow angle, a comparison between maximum and minimum values can thus provide insight into the plunge of the dipole. (iv) The maximum amplitude of the anomaly is strongly dependent on the plunge; a vertical dipole shows a significantly larger anomaly than a horizontal one if all other parameters are the same.

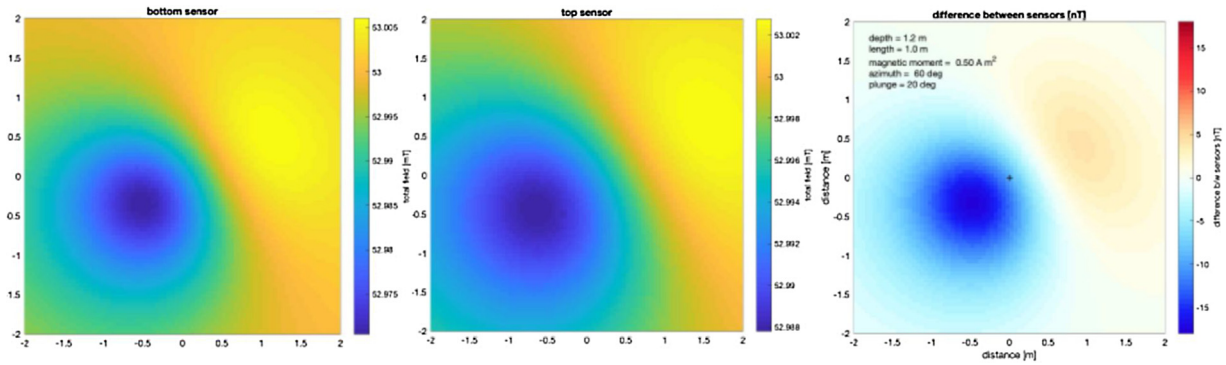


Fig. 2. Total field magnetic data calculated for the bottom sensor (left), top sensor (middle) and the difference between both values (right).

While most of these statements confirm standard geophysical concepts, it highlights that observations of maximum and minimum amplitude, their spatial separation, their orientation on the map, and their width can allow inference of the dipole's depth of burial, azimuth, plunge, and magnetization. The models indicate that hardest to detect will be deep and horizontally oriented firearms with low value of magnetization. As a consequence, the detection limit will depend on the type of firearm (which determines its magnetization), the depth of burial, and the plunge.

2.2. Field data acquisition

Our field study was conducted at a rural test site approximately 25 km Northwest of Pearson International Airport in Ontario, Canada. The soil at the site has been described as a loamy podzol [46]. The site was prepared for a range of forensic investigations in summer 2012. As one component of this investigation, three decommissioned rifles and three decommissioned handguns (for specifics see Table 1) were buried and covered with a 11 × 12 m concrete slab at the site mimicking potential burial at crime sites.

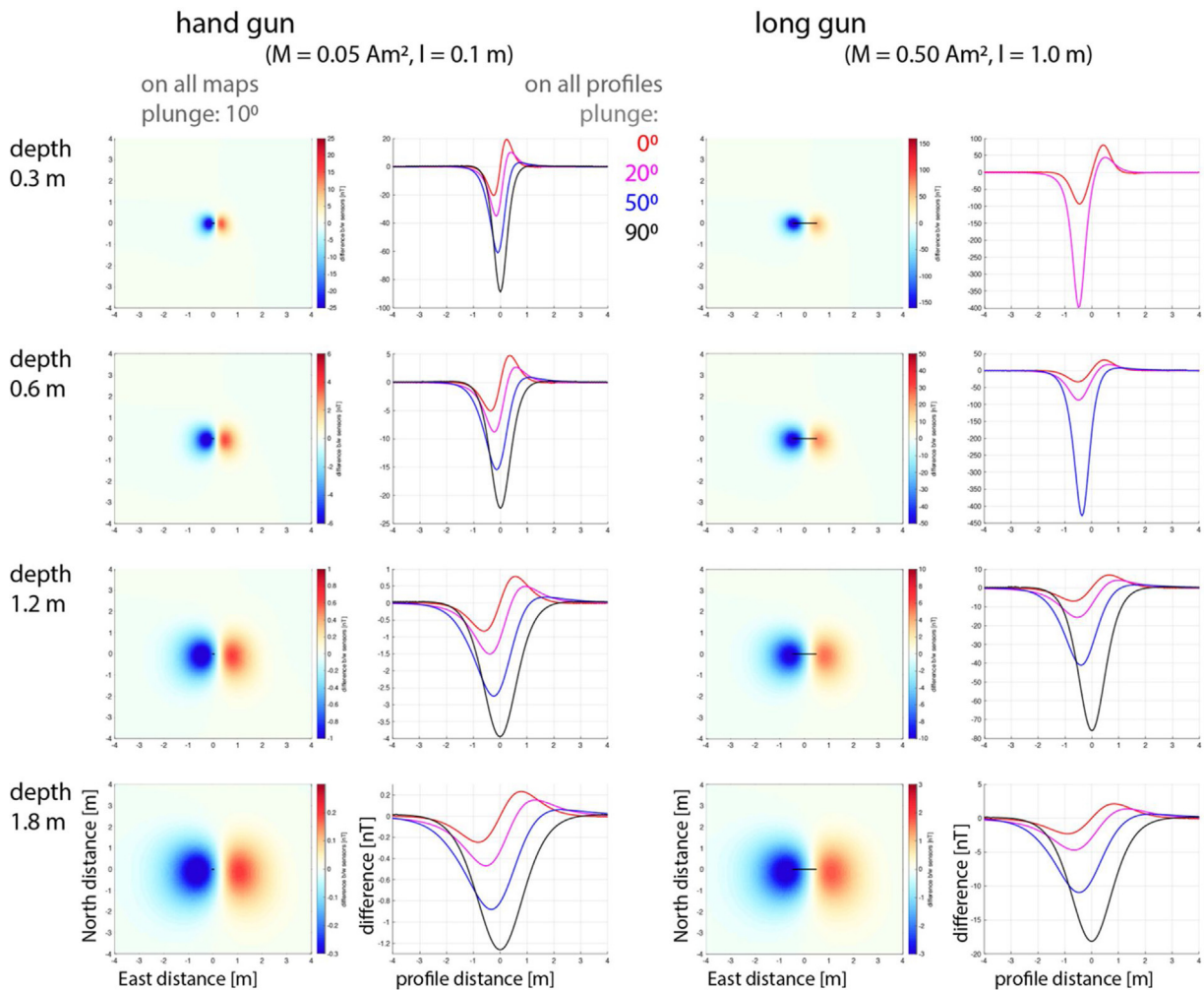








Fig. 3. Representative calculations for two magnetic dipoles (representing different firearms) at varying depths and orientations (see keys).

Table 1
firearms and parameters used to model their magnetic responses.

label	Rs	Rm	Rd	Gs	Gm	Gd
firearm make/model	Remington .12 	Remington .12 	Winchester .22 cal 	Ruger P.89 	Colt .38 	Luger 9mm 
location [m] (in unrotated coordinates)	(2, 2.5)	(5.5, 2.5)	(9, 2.5)	(2, 4.5)	(5.5, 4.5)	(9, 4.5)
depth [m]	0.6	1.2	1.8	0.6	1.2	1.8
azimuth [deg from N]	300	120	120	120	120	120
magnetization [Am^2]	0.4	3.5	1.5	0.08	0.5	1.5
plunge [degrees from horizontal]	-10	10	0	10	0	-30

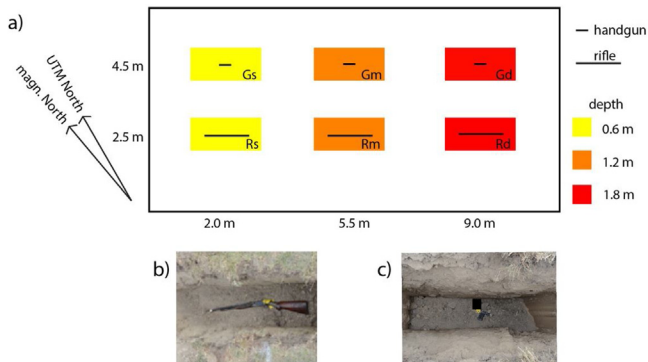


Fig. 4. Schematic sketch map of the site setup with buried decommissioned firearms (a) and examples of on-site buried rifle (b) and handgun (c).

The six burials are separated by 2.0 m–3.5 m, and burial depths are 0.6 m, 1.2 m, and 1.8 m (Fig. 4), with the different burial depths used to assess the depth limitation of the presented method. All firearms were placed horizontally and oriented into the same Northwest–Southeast direction.

Magnetic gradiometric data were collected three times using a GEM-Systems GSM-19GW Overhauser gradiometer which measures the total magnetic field and the vertical gradient with a

nominal sensitivity of 0.0015 nT; however, repeat measurements we took during this survey show a practical repeatability of gradient measurements to 0.15 nT. Positioning was managed by taking point measurements using tape measures as guide. Coarse grids (0.5 m along lines, and lines spaced 1.0 m apart) were collected in June and August 2012 just prior and after burials. A finer grid (0.10 m along profile lines, and lines spaced 0.25 m apart) was measured in October 2015. Sensor elevation was 0.25 m (bottom sensor) and 0.80 m (top sensor) above ground, resulting in a vertical separation of 0.55 m between the sensors. The last survey collected over 3000 data points across the northern half of the slab that overlays the weapons and is the focus of this study.

3. Results

The coarse survey of the unprepared site in June 2012 showed the total field to vary 25 nT between 54,530 nT to 54,555 nT, and gradient readings (difference between sensors) to vary from -7 nT to +14 nT. The finer grid atop the buried firearms in October 2015 showed total field variations of 80 nT between 54,100 nT and 54,180 nT, triple the pre-burial amplitude variation. This overall drop in field strength is consistent with the expected secular variation and magnetic field calculations [45]. The raw difference in total field data (Fig. 5) ranges in value from -37 nT to +21 nT (which approximately corresponds to a gradient of +/- 65 nT/m if

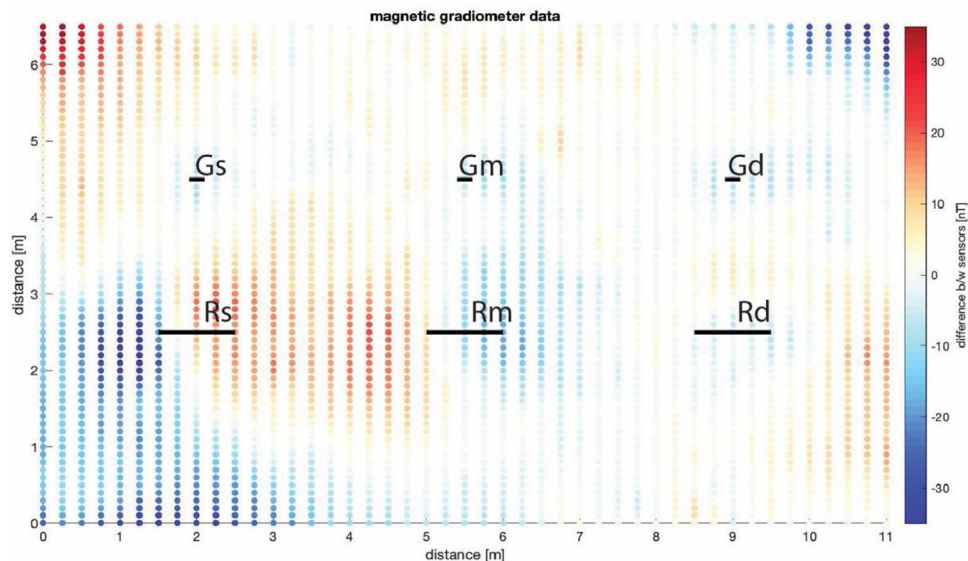


Fig. 5. Gradiometer data collected over buried weapons. Each dot marks a measurement point. As in Fig. 4, the locations of rifles are marked by long lines, while those of handguns are indicated by short lines. The grid is not oriented South-to-North; the y-axis is tilted 20 degrees to the East.

we account for the sensor separation). Some anomalies spatially coincide with the locations of weapons, especially those near grid locations (2, 2.5) and (5.5, 2.5). Dipole anomalies align along the x-axis; this is the known orientation of the firearms. We note that pairs of anomalies measured above firearms seem to be shifted to the left with the negative anomaly appearing above the weapon; only the one at (5.5, 2.5) shows the negative anomaly to the left of the positive. Additional anomalies at the top corners, one positive at (0, 6.5) and the other negative at (11, 6.5), are caused by 8-foot metal bars rammed into the ground as topographic markers, and the anomaly around grid location (2, 0) is caused by a steel drum that was buried outside of the survey grid. A significant positive anomaly along the right edge of the grid around (11, 1) to (11, 2) cannot be linked to a known source. It seems that the visual inspection of the mapped gradiometer data hints at the location of the buried firearms.

4. Discussion

The gradient data (Fig. 5) was gridded (between y distance 1.2 m and 5.8 m to avoid the anomalies at the bottom and the top corners) and rotated (to align with the UTM system) resulting in the map shown in Fig. 6a. We forward modeled synthetic data using the known (E,N,V) locations and azimuth, and adjusted the magnetization and plunge for each weapon until we obtained a reasonable visual fit (Fig. 6b). While the magnetization affects both positive and negative amplitudes, the plunge allows for adjusting the positive and negative amplitudes relative to one another. Fig. 6c shows a map with the residuals which indicates small values around the locations of the firearms; the root mean square (RMS) error value of the residual map is 6 nT. Figs. 6d and 6e show profiles across the burials, RMS misfit values are 6 nT for the rifles and 4 nT for the handguns. The values for all modeling parameters

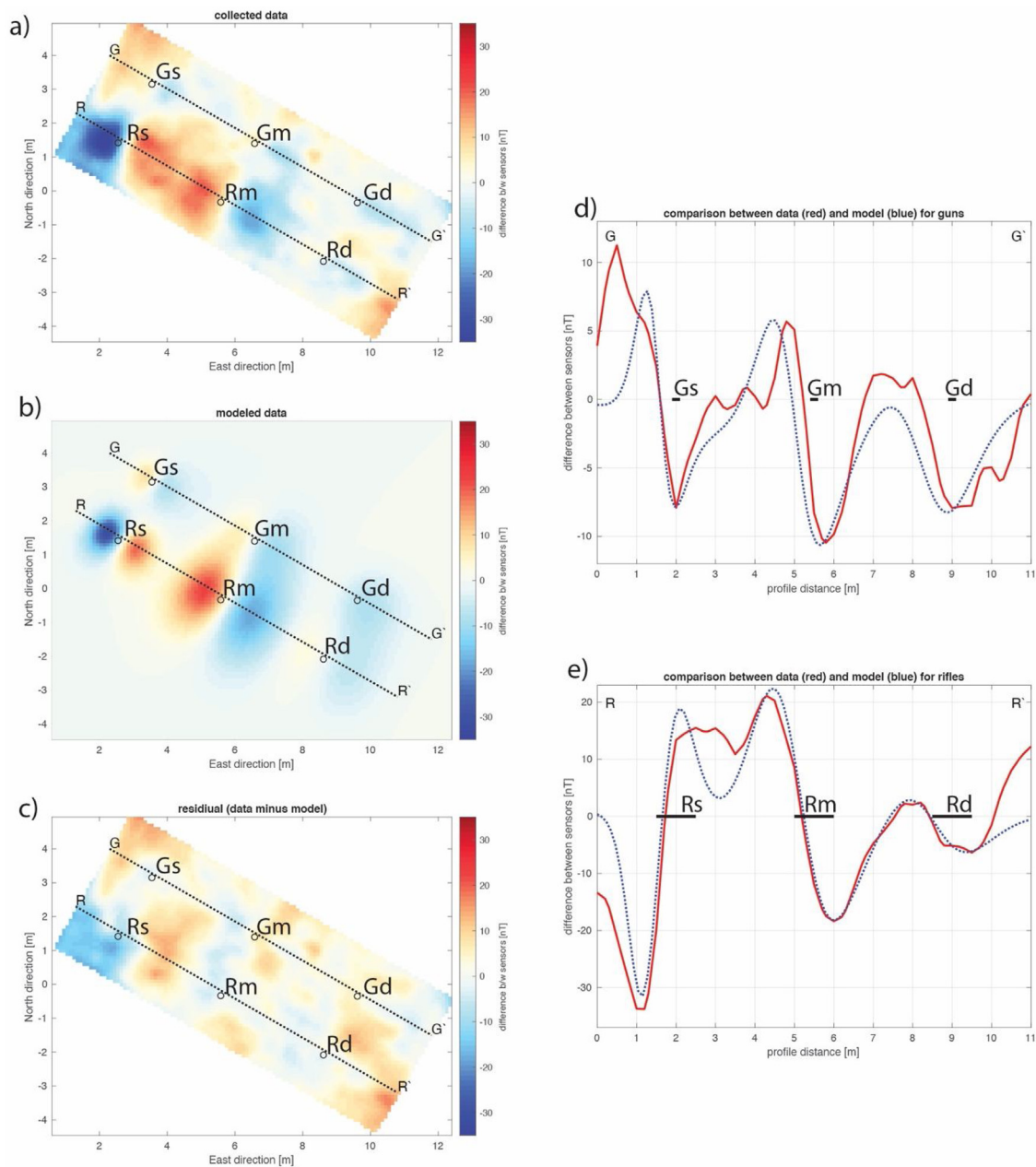


Fig. 6. Comparison of collected and modeled data on maps (top) and along profiles (bottom). Dotted lines in the top panels show the location of the profiles in the bottom panels. Locations of firearms are denoted by circles on the maps and by lines on the profiles. (a) gridded field data, (b) modeled data, (c) residual, (d) measured and modeled profiles crossing handguns, (e) measured and modeled profiles crossing rifles.

are summarized in Table 1. Magnetic models are non-unique, meaning there is some flexibility in our modeling results, yet they allow us to state several observations.

The modeled map shows clearly separate responses for the shallow firearms but stretched anomalies for encompassing pairs of deeper ones, because their anomalies overlap spatially at the surface. It also makes it obvious that the positive-negative anomaly pairs for each handgun (along the top profile line) are closer together than those for each rifle (along the bottom profile line). The shallow firearms may be better fitted by broader anomalies, which would mean that they were buried deeper and had larger magnetization than our model assumes. It could be that the assumption of a thin dipole is less adequate for the shallow burials. We note that the values of magnetization are smallest for the shallow firearms.

Anomalies for the three rifles are above ± 5 nT, meaning they should fall above the noise level and thus be detectable in a blind survey. The shallow and intermediate handguns are around that amplitude, and for the deep handgun we model a plunge of 30 degrees which, as shown in the modeling section above, makes for larger amplitudes than if the handgun was horizontal. The burials were dug using an excavator which scoops a curved surface so it is possible that the weapon did not rest perfectly horizontal, and careless infilling could have rotated the weapon further. Alternatively, the magnetic field of this gun is distorted by a larger scale anomaly centered outside the measuring area east of (11, -3) where we observe a local maximum. A similar argument could be made to explain the modeled plunge of rifle Rs; however, the overall weakening and broadening of its maximum could also be caused by different parts of the stock which give rise to individual magnetic fields that superpose.

Our data collection was done at very close spacing, and it took us about 5 h to collect the 6.5×11 m area. The modeling results (Fig. 3) indicate that the half-width of anomalies for firearms at shallow burials requires a mesh not coarser than 0.25 m to ensure that at least one measurement point falls within that half-width. Measured anomalies for the rifles seem broader, but the measured anomalies for the handguns are spatially concentrated, thus a spacing of 0.25 m can be suggested. We did point measurements, and an automated data collection ("walking mode") would speed up the data collection, but at the expense of higher noise and less accurate positioning.

To our knowledge this is the first study which investigates a selection of firearms buried to 1.8 m at a controlled site. Three publications address different surveys on a site in Florida to investigate a large range of weapons, including 16 firearms which were reburied every 0.05 m starting at 0.20 m. When using the Schonstedt GA-72Cd magnetic gradiometer [2], and relying on the audio signal it produces under a strong gradient, the firearms detection limit was 0.25 m to 0.75 m depending on the weapon's size. When mapping the ground conductivity using a Geonics EM-38 conductivity meter [25] burials between 0.30 m and 0.75 m could be detected when relying on a threshold of >1 mS. Searching with a Fisher M-97 metal detector [25] gave an audible response for firearms no deeper than 0.30 m to 0.55 m. Another study done in the UK [28] included two replica handguns which were buried and surveyed with a ground-penetrating radar, a conductivity meter, and a magnetic gradiometer, specifically a Geoscan FM256 fluxgate magnetic gradiometer which measures the vertical component of the magnetic field at two elevations 0.5 m apart. The researchers mapped on a very fine grid (0.125 m between measurements) and found that the replica handguns had "weak" (= difficult to interpret) anomalies. They noted that the material of these replicas is a mixture of non-magnetic alloys and some steel; probably this material was not representative for the magnetic properties of real firearms. A third study, also in the UK [29],

compared the success of different types of equipment in detecting various objects, including one replica handgun, buried at 0.15 m depth and covered with concrete patio slabs. The testing equipment included a Geonics FM15 fluxgate vertical gradiometer and a Gem Systems GSM-40 K vapour gradiometer. Survey lines were 0.25 m apart with closer data spacing along lines; the collected data was despiked, gridded, and detrended for visual target detection. The survey found large standard deviations in the data with the potassium magnetometer having a better success rate than the fluxgate magnetometer; however metal detectors, magnetic susceptibility equipment, and ground-penetrating radar were all found to be superior on grass, and magnetic susceptibility was better than the potassium magnetometer on the patio setting. All these studies investigated shallow burials less than 1 m deep, and in comparison we provide a better detection limit since we can image large firearms down to 1.8 m.

One of our study objectives was to determine the maximum depth to which a magnetic gradiometer may detect buried firearms. We applied forward modeling to provide an estimate for burial depth (as suggested in [29]) and compared this to field data. We found that the amplitude of magnetic anomalies drop from ± 20 nT for large weapons at 0.6 m depth to ± 2 nT for handguns buried at 1.8 m depth with variations depending on the plunge of the buried item. The detection limit will be dependent on the accuracy of measurements as well as the amplitude of magnetic spatial variations of the particular site; the magnetic anomaly caused by the object should surpass both for anomalies to be detected. At this site a blind study would probably miss the deep handgun because its anomaly is smaller than the variations from the soil. One might be able to increase the detection limit if one subjected the data to advanced analysis methods which compares the data to a range of possible anomaly patterns derived by the forward model.

5. Conclusion

Our study shows that gradient magnetometry is able to detect a variety of firearms buried to 1.8 m. Horizontally buried firearms produce smaller anomalies, while even slight plunges will significantly enhance either the positive or negative anomaly, and vertical burials can increase the amplitude measured at the surface several times. To improve field application of magnetic gradiometry for locating buried weapons such as guns, we suggest that measurements should involve running a coarser sweep of the area to catch large scale anomalies. This has to be followed by surveying on a grid measuring no wider than at 0.25 m spacing. The spacing between the gradiometer sensors should be small with the lower sensor and upper sensor no higher than 0.25 m and 0.80 m above the surface respectively.

Our study is limited by magnetic background variations owing to the soil and site preparation. The unprepared site showed significant magnetic variation. A historical soil report [46] notes that the soil in the county has been derived by weathering and glacial activity from underlying shale bedrock which contains significant amounts (~5%) of iron oxide. The site was not intended for magnetic surveys of firearms but set up by law enforcement as a training site to detect buried bodies, containers, and firearms. Metal markers, and the burial of other objects (e.g., metal drums) give rise to large magnetic anomalies that interfered with our survey. It can be assumed that a site with less background magnetization would be more amenable to detecting firearms.

Research at controlled field sites has made important contributions to our ability to detect buried firearms, and our study also answers to the need for testing of equipment at such sites. However, we would like to stress modeling as an additional aspect of forensic research that may assist in the selection of a suitable

method given a certain environment or a specific target. When appropriate parameters are known, modeling can allow us to test a much larger data space than one field site can provide. We may simulate different environmental conditions (for example variations in ground conductivity at one site) or different geologic settings and how these may influence our detection limits. Our study offers a simple model for firearms in magnetic searches.

Magnetometry is an underused method in forensic searches. Our results indicate that magnetic gradiometers could be useful in finding clandestine weapons, for example if disposed in a grave or shallow water body. We recommend further studies to extend findings of this study by testing the effects of varying soil types, consolidation and other geologic and geomorphological properties on measured anomaly and also to compare vertical and tilted weapon burials with the horizontal and subhorizontal burials investigated in this study.

CRedit authorship contribution statement

Elijah Achuoth Deng: Formal analysis, Visualization, Writing - original draft. **Kennedy O. Doro:** Data curation, Formal analysis, Supervision, Validation, Writing - review & editing. **Carl-Georg Bank:** Conceptualization, Funding acquisition, Investigation, Methodology, Project administration, Software, Supervision, Visualization.

Declaration of Competing Interest

None.

Acknowledgements

This work was supported by the Research Opportunities Program in the Faculty of Arts and Science at the University of Toronto. The authors thank the team who prepared the site, the property owners who granted access, several undergraduate students who helped collect data, and the anonymous reviewers for their very thorough and helpful comments.

References

- [1] J.K. Pringle, A. Ruffell, J.R. Jervis, L. Donnelly, J. McKinley, J. Hansen, R. Morgan, D. Pirrie, M. Harrison, The use of geoscience methods for terrestrial forensic searches, *Earth. Rev.* 114 (1) (2012) 108–123, doi:<http://dx.doi.org/10.1016/j.earscirev.2012.05.006>.
- [2] M.M. Rezos, J.J. Schultz, R.A. Murdock, S.A. Smith, Utilizing a magnetic locator to search for buried firearms and miscellaneous weapons at a controlled research site, *J. Forensic Sci.* 56 (5) (2011) 1289–1295, doi:<http://dx.doi.org/10.1111/j.1556-4029.2011.01802.x>.
- [3] D.P. Auchie, Expert scientific evidence in Court: the legal considerations, in: K. Ritz, L. Dawson, D. Miller (Eds.), *Criminal and Environmental Soil Forensics*, Springer, Dordrecht, 2009, pp. 13–31, doi:http://dx.doi.org/10.1007/978-1-4020-9204-6_2.
- [4] A. Curran, P. Prada, K. Furton, Canine human scent identifications with post-blast debris collected from improvised explosive devices, *Forensic Sci. Int.* 199 (1) (2010) 103–108, doi:<http://dx.doi.org/10.1016/j.forsciint.2010.03.021>.
- [5] A. Ruffell, J. McKinley, *Forensic geomorphology*, *Geomorphology* 206 (2014) 14–22, doi:<http://dx.doi.org/10.1016/j.geomorph.2013.12.020>.
- [6] M. Harrison, L.J. Donnelly, Locating concealed homicide victims: developing the role of geoforensics, in: K. Ritz, L. Dawson, D. Miller (Eds.), *Criminal and Environmental Soil Forensics*, Springer, Dordrecht, 2009, pp. 197–219, doi:http://dx.doi.org/10.1007/978-1-4020-9204-6_13.
- [7] P.J. Fenning, L.J. Donnelly, Geophysical techniques for forensic investigation, *Geol. Soc. London Spec. Publ.* 232 (1) (2004) 11–20, doi:<http://dx.doi.org/10.1144/GSL.SP.2004.232.01.03>.
- [8] M. Everett, *Near-surface Applied Geophysics*, Cambridge University Press, 2013, doi:http://dx.doi.org/10.1017/CBO9781139088435milsom_403_pg.
- [9] M. Fedi, F. Cella, G. Florio, M. La Manna, V. Paoletti, *Geomagnetometry for archaeology*, in: N. Masini, F. Soldovieri (Eds.), *Sensing the Past - from Artifact to Historical Site*, Springer, Cham, Switzerland, 2017, pp. 203–230, doi:http://dx.doi.org/10.1007/978-3-319-50518-3_10.
- [10] N. Wahlstroem, *Modeling of Magnetic Fields and Extended Objects for Localization Applications*. PhD Thesis, Linköping University, Linköping Sweden, 2015 236 pg. 2015. <https://theses.eurasip.org/theses/642/modeling-of-magnetic-fields-and-extended-objects/> (accessed 19 May 2020).
- [11] J. Milsom, A. Eriksen, *Field Geophysics*, fourth ed., Wiley, Hoboken, 2011, doi:http://dx.doi.org/10.1002/9780470972311_304_pg.
- [12] A. Ruffell, B. Kullessa, Application of geophysical techniques in identifying illegally buried toxic waste, *Environ. Forensics* 10 (3) (2009) 196–207, doi:<http://dx.doi.org/10.1080/15275920903130230>.
- [13] M. Solla, B. Riveiro, M.X. Álvarez, P. Arias, Experimental forensic scenes for the characterization of ground-penetrating radar wave response, *Forensic Sci. Int.* 220 (1) (2012) 50–58, doi:<http://dx.doi.org/10.1016/j.forsciint.2012.01.025>.
- [14] M.M. Cavalcanti, M.P. Rocha, M.L.B. Blum, W.R. Borges, The forensic geophysical controlled research site of the University of Brasilia, Brazil: results from methods GPR and electrical resistivity tomography, *Forensic Sci. Int.* 293 (2018) 101.e1–101.e21, doi:<http://dx.doi.org/10.1016/j.forsciint.2018.09.033>.
- [15] J.K. Pringle, J. Jervis, J.P. Cassella, N.J. Cassidy, Time-lapse geophysical investigations over a simulated urban clandestine grave, *J. Forensic Sci.* 53 (6) (2008) 1405–1416, doi:<http://dx.doi.org/10.1111/j.1556-4029.2008.00884.x>.
- [16] D.C. Nobes, The search for “Yvonne”: a case example of the delineation of a grave using near-surface geophysical methods, *J. Forensic Sci.* 45 (3) (2000) 715–721, doi:<http://dx.doi.org/10.1520/JFS14756J>.
- [17] V. Di Fiore, G. Cavuoto, M. Punzo, D. Tarallo, M. Casazza, S.M. Guarriello, M. Lega, Integrated hierarchical geo-environmental survey strategy applied to the detection and investigation of an illegal landfill: a case study in the Campania Region (Southern Italy), *Forensic Sci. Int.* 279 (2017) 96–105, doi:<http://dx.doi.org/10.1016/j.forsciint.2017.08.016>.
- [18] J.K. Pringle, M. Giubertoni, N.J. Cassidy, K.D. Wisniewski, J.D. Hansen, N.T. Linford, R.M. Daniels, The use of magnetic susceptibility as a forensic search tool, *Forensic Sci. Int.* 246 (2015) 31–42, doi:<http://dx.doi.org/10.1016/j.forsciint.2014.10.046>.
- [19] D. Donskoy, A. Reznik, A. Zagrai, A. Ekimov, Nonlinear vibrations of buried landmines, *J. Acoust. Soc. Am.* 117 (2) (2005) 690–700, doi:<http://dx.doi.org/10.1121/1.1850410>.
- [20] M. Connor, D.D. Scott, Metal detector use in archaeology: an introduction, *Hist. Archaeol.* 32 (4) (1998) 76–85 <https://www.jstor.org/stable/25616646>. Accessed 10 May 2020.
- [21] C.A. Dionne, J.J. Schultz, R.A. Murdock, S.A. Smith, Detecting buried metallic weapons in a controlled setting using a conductivity meter, *Forensic Sci. Int.* 208 (1) (2011) 18–24, doi:<http://dx.doi.org/10.1016/j.forsciint.2010.10.019>.
- [22] S. Dogru, L. Marques, Estimating depth of buried metallic objects, 17th IEEE SENSORS Conference, New Delhi, India, 2018, doi:<http://dx.doi.org/10.1109/ICSENS.2018.8589731>.
- [23] A.M. Kaneko, G. Endo, G.E. Fukushima, Landmine buried depth estimation by curve characterization of metal mine detector signals, *IEEE/RSJ International Conference on Intelligent Robots and Systems*, Tokyo, Japan, 2013, doi:<http://dx.doi.org/10.1109/IROS.2013.6697127>.
- [24] F. Alfouzan, B. Zhou, K. Bakkour, M. Alyousif, Detecting near-surface buried targets by a geophysical cluster of electromagnetic, magnetic and resistivity scanners, *J. Appl. Geophys.* 134 (2016) 55–63, doi:<http://dx.doi.org/10.1016/j.jappgeo.2016.08.006>.
- [25] M.M. Rezos, J.J. Schultz, R.A. Murdock, S.A. Smith, Controlled research utilizing a basic all-metal detector in the search for buried firearms and miscellaneous weapons, *Forensic Sci. Int.* 195 (1) (2010) 121–127, doi:<http://dx.doi.org/10.1016/j.forsciint.2009.12.003>.
- [26] A. Lukasi, M. Szuszkiewicz, T. Magiera, Impact of artifacts on topsoil magnetic susceptibility enhancement in urban parks of the Upper Silesian conurbation datasets, *J. Soils Sediments* 15 (2015) 1836–1846, doi:<http://dx.doi.org/10.1007/s11368-014-0966-5>.
- [27] P. Czippott, *Stand-off Detection and Tracking of Concealed Weapons Using Magnetic Tensor Tracking, Final Activities Report, Quantum Magnetics*, San Diego, USA, 2001 <https://www.ncjrs.gov/pdffiles1/nij/grants/189583.pdf>. Accessed 09 May 2020.
- [28] T. Richardson, P. Cheetham, The effectiveness of geophysical techniques in detecting a range of buried metallic weapons at various depths and orientations, *Geol. Soc. London Spec. Publ.* 384 (2013) 253–266, doi:<http://dx.doi.org/10.1144/SP384.18>.
- [29] J.D. Hansen, J.K. Pringle, Comparison of magnetic, electrical and ground penetrating radar surveys to detect buried forensic objects in semi-urban and domestic patio environments, *Geol. Soc. London Spec. Publ.* 384 (2013) 229–251, doi:<http://dx.doi.org/10.1144/SP384.13>.
- [30] G. Desvignes, A. Tabbagh, D. Benech, The determination of the depth of magnetic anomaly sources, *Archaeol. Prospect.* 6 (1999) 85–105, doi:[http://dx.doi.org/10.1002/\(SICI\)1099-0763\(199906\)6:2<85::AID-ARP119>3.0.CO;2-I](http://dx.doi.org/10.1002/(SICI)1099-0763(199906)6:2<85::AID-ARP119>3.0.CO;2-I).
- [31] K. Davis, Y. Li, M. Nabighian, Automatic detection of UXO magnetic anomalies using extended Euler deconvolution, *Geophysics* 75 (3) (2010) G13–G20, doi:<http://dx.doi.org/10.1190/1.3375235>.
- [32] B. Oruc, Location and depth estimation of point-dipole and line of dipoles using analytic signals of the magnetic gradient tensor and magnitude of vector components, *J. Appl. Geophys.* 70 (2010) 27–37, doi:<http://dx.doi.org/10.1016/j.jappgeo.2009.10.002>.
- [33] A. Salem, S. Williams, J. Fairhead, D. Ravat, R. Smith, Tilt-depth method: a simple depth estimation method using first-order magnetic derivatives, *Lead. Edge* 26 (12) (2007) 1502–1505, doi:<http://dx.doi.org/10.1190/1.2821934>.
- [34] D. Larson, A. Vass, M. Wise, Advanced scientific methods and procedures in the forensic investigation of clandestine graves, *J. Contemp. Crim. Justice* 27 (2) (2011) 149–182, doi:<http://dx.doi.org/10.1177/1043986211405885>.

- [35] S. Breiner, Application Manual for Portable Magnetometers, GeoMetrics, San Jose, California, USA, 1999 58 pg. <https://www.geometrics.com/resources> (accessed 18 May 2020).
- [36] C. Schlinger, Magnetometer and gradiometer surveys for detection of underground storage tanks, *Environ. Eng. Geosci.* 27 (1) (1990) 37–50, doi: <http://dx.doi.org/10.2113/gseegeosci.xxvii.1.37>.
- [37] D. Argote, A. Tejero, R. Chávez, P. López, R. Bravo, 3D modelling of magnetic data from an archaeological site in north-western Tlaxcala state, Mexico, *J. Archaeol. Sci.* 36 (8) (2009) 1661–1671, doi: <http://dx.doi.org/10.1016/j.jas.2009.03.004>.
- [38] V. Kravchinsky, D. Hnatyshin, B. Lysa, W. Alemie, Computation of magnetic anomalies caused by two-dimensional structures of arbitrary shape: derivation and Matlab implementation, *Geophys. Res. Lett.* 46 (2019) 7345–7351, doi: <http://dx.doi.org/10.1029/2019GL082767>.
- [39] A. Schettino, A. Ghezzi, P. Pierantoni, Magnetic field modelling and analysis of uncertainty in archaeological geophysics, *Archaeol. Prospect.* 26 (2019) 137–153, doi: <http://dx.doi.org/10.1002/arp.1729>.
- [40] M. Geng, X. Hu, H. Zhang, S. Liu, 3D inversion of potential field data using a marginalizing probabilistic method, *Geophysics* 83 (5) (2019) G93–G106, doi: <http://dx.doi.org/10.1190/GEO2016-0683.1>.
- [41] C. Rücker, T. Günther, F. Wagner, pyGIMLI: an open-source library for modelling and inversion in geophysics, *Comput. Geosci.* 109 (2017) 106–123, doi: <http://dx.doi.org/10.1016/j.cageo.2017.07.011>.
- [42] K. Seleznyova, M. Strugatsky, J. Kliava, Modelling the magnetic dipole, *Eur. J. Phys.* 37 (2) (2016) 025203, doi: <http://dx.doi.org/10.1088/0143-0807/37/2/025203>.
- [43] K. Seleznyova, M. Strugatsky, J. Kliava, Erratum: modelling the magnetic dipole (2016 *Eur. J. Phys.* 37 025203), *Eur. J. Phys.* 37 (3) (2016) 039601, doi: <http://dx.doi.org/10.1088/0143-0807/37/3/039601>.
- [44] K. Seleznyova, M. Strugatsky, J. Kliava, Reply to Comment on 'modelling the magnetic dipole', *Eur. J. Phys.* 37 (5) (2016) 058002, doi: <http://dx.doi.org/10.1088/0143-0807/37/5/058002>.
- [45] NOAA, Magnetic Field Calculators, (2019) <https://www.ngdc.noaa.gov/geomag/calculators/magcalc.shtml>. (accessed 20 May 2019).
- [46] D. Hoffman, N. Richards, Soil Survey of Peel County, Report No. 18 of the Ontario Soil Survey, Experimental Farms Service, Canada Dept. of Agriculture, Ottawa, Canada, 1953 84 pg. <http://sis.agr.gc.ca/cansis/publications/surveys/on/on18/index.html> (accessed 19 May 2020).